A Priori Inference of Cross Reactivity for Drug-Targeted Kinases

Ariel Fernández*,† and Sridhar Maddipati‡

Department of Bioengineering, Rice University, Houston, Texas 77005, and School of Chemical Engineering, Purdue University, West Lafayette, Indiana 47906

Received February 14, 2006

Kinases are central targets for drug-based treatment of diseases such as cancer, diabetes, and arthritis. Progress in drug development faces challenges due to undesirable cross reactivity and difficulties in modulating selectivity, both consequences of fold conservation. Here we present a structure-based predictor of cross reactivity and validate it against affinity fingerprinting of the kinases and our own drug redesign geared at sharpening the inhibitory impact. The predictor assesses protein environments of binding pockets, compares patterns of packing defects, and introduces a packing distance in kinase space. This metric is conclusively shown to be equivalent to pharmacological distance generated by comparing affinity fingerprintings. Our packing distance metric is further extended to infer cross reactivity over all human tyrosine kinases. This tool should prove useful to target clinically relevant regions of the pharmacokinome, as our experimental assays reveal.

Introduction

Protein kinases are quintessential signal transducers, and thus their inhibition becomes a central strategy to block specific signaling pathways, as often needed for therapeutic reasons.[1−6] However, recent high-throughput screening data reveals that most kinase inhibitors of pharmacological relevance exhibit high cross reactivity.[7] Thus, we ultimately aim at using molecular design to modulate cross reactivity in order to sharpen the impact of a new generation of drugs on targets of clinical relevance for therapeutic purposes. This is a challenging problem since the extent of structural conservation of kinases, especially at the primary (ATP-) binding sites, is staggering.[3,7] Cross reactivity does not necessarily hinder activity, and it might even be desirable in particular therapeutic contexts, i.e., when the inhibitory impact spreads exclusively over targets of clinical relevance, but it frequently leads to toxic side effects.[2]

Here we report on the a priori prediction of cross reactivity based on structural attributes of kinases. Such inferences require that we assess differences in the packing of the ATP-binding pockets. Specifically, we focus on the pattern of packing defects in the form of poorly wrapped or underdehydrated backbone hydrogen bonds, named *dehydrons*.[8,9] Dehydrons are functionally critical because they are indicators of protein interactivity, or markers for protein−ligand association,[8] and thus constitute a decisive factor in macromolecular recognition. The emphasis on dehydrons stems from two facts: (a) dehydrons promote the removal of surrounding water, and therefore, may anchor ligands that contribute to their dehydration upon association with the protein[8] and (b) dehydron patterns are not conserved across paralogs.[9]

Thus, by comparing dehydron patterns, we introduce a "packing distance" in kinase space. As shown below, this structure-based metric correlates linearly with a pharmacological distance, implying that cross reactivity is essentially dictated by packing similarity. Our pharmacological distance between kinases is based on a comparison of their respective affinity fingerprinting that arises from a screening of the kinases against an assortment of inhibitory compounds.[10]

The structure-based predictor is validated by contrasting the packing distance between kinases against a benchmark metric constructed from experimental cross-reactivity profiles of drug inhibitors.[7] This study introduces a methodology to assess a priori the extent of target selectivity as a means to guide drug design.

Results

Kinase Inhibitors as Dehydron Wrappers. Protein dehydrons are critical markers of protein interactivity since they promote their own dehydration as a means to enhance and stabilize the electrostatic contribution to the hydrogen bond.[11] Dehydrons may be identified from protein structure by quantifying the extent of intramolecular desolvation of the hydrogen bonds, as described in the Methods section. The extent of intramolecular dehydration is given by the number of "*wrapping*" nonpolar groups contained within a defined microenvironment around the hydrogen bond (Methods). Thus, a ligand designed to wrap a protein dehydron contributes with some nonpolar groups to the desolvation domain of the hydrogen bond upon association with the protein.[8]

The interfaces of the nonredundant 814 protein−inhibitor PDB complexes were examined to determine whether inhibitors were "dehydron wrappers", that is, whether nonpolar groups of inhibitors penetrated the desolvation domain of dehydrons upon association. This feature was found in 631 complexes, and *invariably* found in the 488 complexes whose binding cavities presented average or no surface hydrophobicity. This fact is illustrated in Figure 1a, where imatinib, Gleevec,[2] an inhibitor of C-Kit kinase,[12−14] is shown to be an exogenous wrapper of the packing defects in the ATP-binding site.

Hydrophobic interactions between inhibitors and exposed nonpolar moieties in the protein tend to foster promiscuity, as surface nonpolar residues are highly conserved.[15] That is indeed the case with staurosporine (Figure 1b), whose extensive cross reactivity renders it therapeutically useless.[7] On the other hand, dehydrons are not conserved across paralogs,[9] suggesting their role as selectivity filters for drug design.

* Corresponding author. Phone: 713-348-3681. Fax: 713-348-3699. E-mail: arifer@rice.edu.
† Rice University.
‡ Purdue University.

10.1021/jm060163j CCC: $33.50
Published on Web 05/03/2006

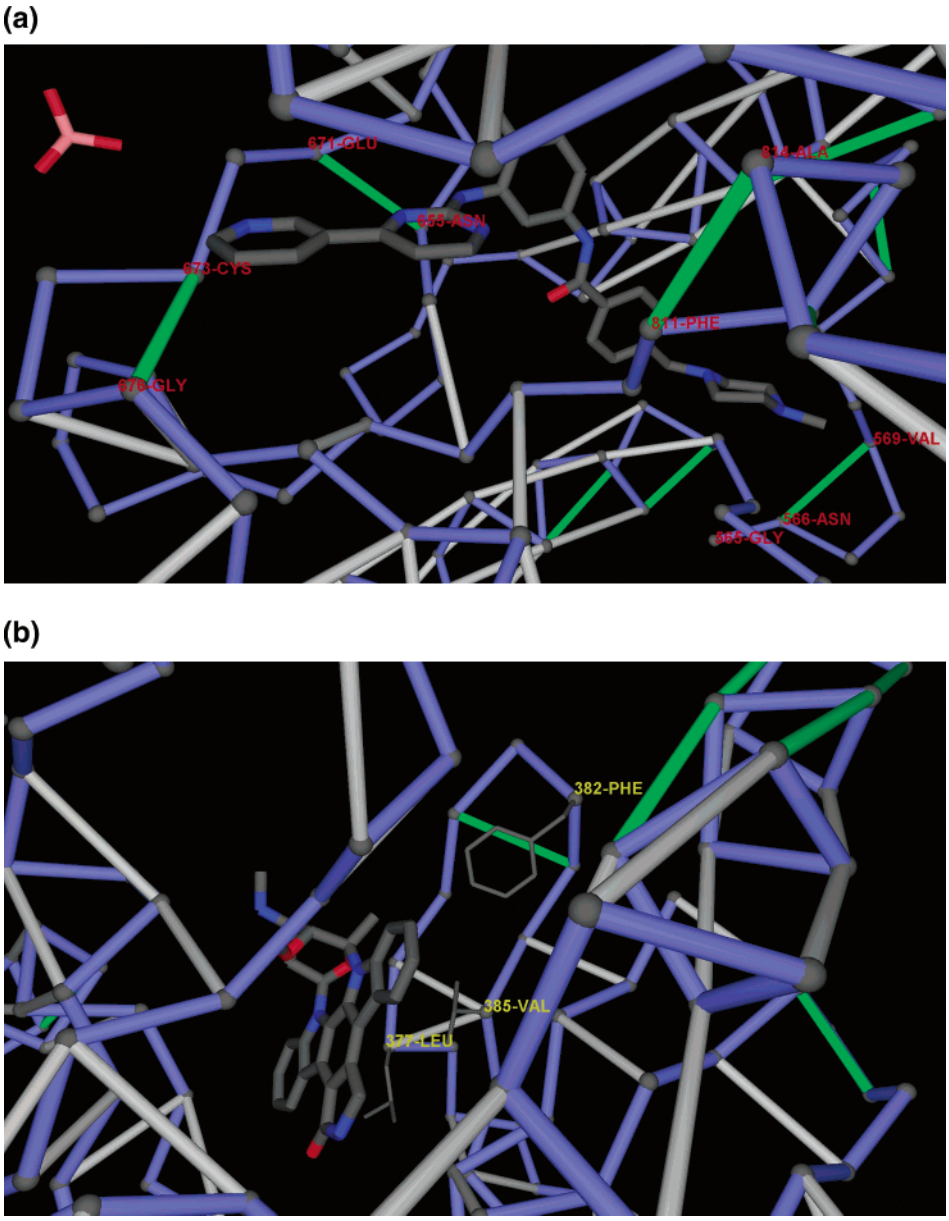

Figure 1. (a) Wrapping of ATP-binding site for the C-Kit kinase. There are four dehydrons in the pocket that are wrapped by the Gleevec molecule upon association, as reported in the PDB complex (PDB.1T46): Asn566−Val569; Asn655−Glu671; Cys673−Gly676; Phe811−Ala814. The protein chain backbone is represented by blue virtual bonds joining α-carbons, well-wrapped backbone hydrogen bonds are shown as light gray segments joining the α-carbons of the paired residues, and dehydrons are shown as green segments. The figure shows the cavity in detail, the pattern of packing defects, and the inhibitor positioned as a dehydron wrapper. (b) Binding mode of staurosporine illustrated by its association to Syk kinase (PDB.1XBC). Staurosporine does not wrap the packing defects of Syk; rather, it is engaged in hydrophobic associations with the highly conserved nonpolar residues Leu377, Phe382, and Val385, all located on the Syk surface.

Packing Distance vs Pharmacological Distance. To support this concept, a "packing distance" is defined by comparing the different packing arrangements of the hydrogen bonds wrapped by a composite of 17 inhibitors that bind individually at the ATP site. The region wrapped by the composite is termed "hull". The inhibitors are selected from a pool of 20 that have been independently assayed for cross reactivity against a set of 113 kinases.[7] Three inhibitors, staurosporine, SU11248 (sunitinib malate)[16] and EKB569 (3-cyanoquinoline)[17] were excluded since PDB protein−inhibitor complexes revealed a mode of anchoring based on hydrophobic interactions (cf. Figure 1b) and, consequently, leading to high promiscuity, as indicated above. This promiscuity would mask selective features in the pharmacological distance matrix. The composite is the reunion of inhibitors in their positions within their complexes after 3D-alignment of the respective protein backbones (Figure 2) Packing differences between hulls may be turned into a distance between kinases by following four steps: (a) alignment of hydrogen-bond matrices; (b) derivation of dehydron matrices that inherit their alignment from step a; (c) restricting dehydron matrices to the hulls; and (d) computing the Hamming distance between restricted dehydron matrices.

To compute the packing distance matrix (PDM) we selected the 32 kinases reported in PDB for which affinity fingerprinting is available through screening against the 17 drug inhibitors.[7] The PDM is displayed in Figure 3a. This result is contrasted with a pharmacological distance matrix (Figure 3b) obtained by computing the Euclidean distance between affinity vectors in $\mathbf{R}^{17}$ with entries given in −ln scale (or dimensionless ΔG/

Figure 2. Construction of the inhibitor composite by alignment of kinases crystallized in complex with their ligands and superimposition of the ligand molecules. The first two iterations of the 17 needed to build the inhibitor composite are shown. (a) The Gleevec+Syk complex (PDB.1XBB). (b) Superposition of complexes Gleevec+Syk (purple protein backbone) and SB203580+p38MAPK (blue protein backbone) resulting after alignment of the respective protein backbones.

RT units; ΔG = Gibbs free energy change associated with binding, R = universal gas constant, T = absolute temperature).

By plotting packing versus pharmacological distance (Figure 3c) for each pair of kinases reported in PDB and experimentally assayed for affinity against 17 drug ligands, we establish a strong correlation ($R^2 = 0.9028$). This correlation reveals that the dehydron pattern is in fact an operational selectivity filter for drug design. Thus, proteins with similar packing have similar

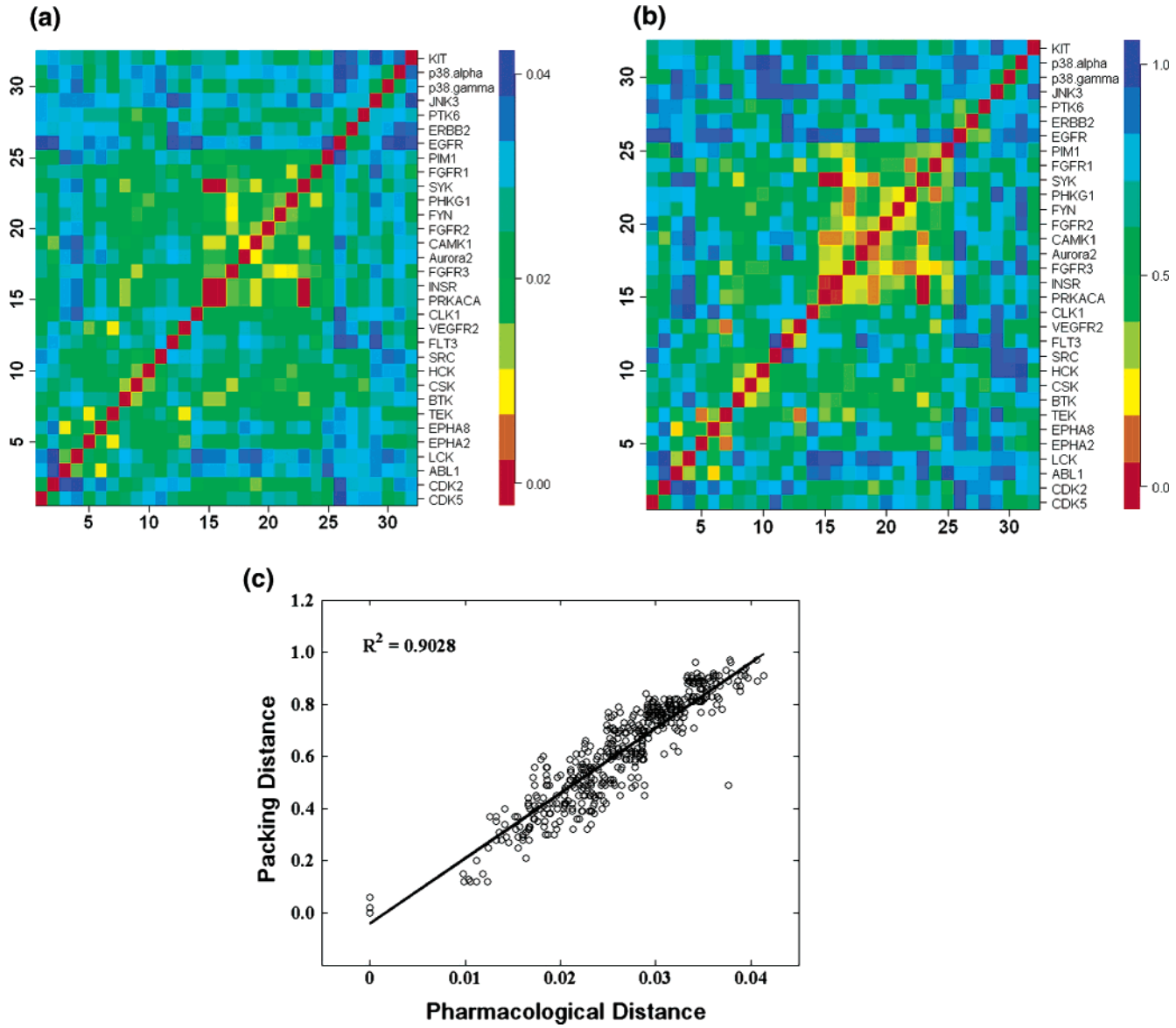

Figure 3. (a) Packing distance matrix corresponding to all PDB-reported proteins that have been independently fingerprinted in affinity assays. Packing distances are determined by comparing the packing of the hulls of the composite inhibitor in different proteins. The packing distance is the Hamming distance between dehydron matrices restricted to the residues forming the hydrogen-bond microenvironments within the hull. (b) Pharmacological distance matrix restricted to PDB-reported proteins assayed for affinity by screening them against 17 drug-based inhibitors. This matrix is obtained by computing the Euclidean distance between affinity vectors in $\mathbf{R}^{17}$ with entries given in $-\ln$ scale. (c) Correlation between packing distance and pharmacological distance for all pairs constructed from the pool of 32 PDB-reported kinases fingerprinted for affinity against 17 drugs.

affinity patterns, and conversely, significant packing differences make targets pharmacologically different.

Packing Distances across the Tyrosine Kinome. Having validated the packing distance as a marker for drug cross reactivity, we are in a position to expand the packing comparisons to the entire tyrosine kinome (93 kinases), of direct relevance to cancer therapy.[14,15] Our analysis is not constrained to PDB-reported tyrosine kinases (19 out of 93, Table 1), since dehydrons may be directly inferred from sequence.[9] Such inferences make use of a strong correlation between the extent of wrapping and the so-called disorder score,[9,18] an accurate sequence-based attribute that indicates the propensity of a peptide-chain window to be disordered [18] (Methods). Thus, the correlation reveals that native disorder arises essentially from the impossibility to pack intramolecular hydrogen bonds.

The disorder score, λ_D, for individual residues may be directly obtained from the plot generated by PONDR, the predictor for native disorder,[18] where $\lambda_D = 1$ indicates certainty of disorder and $\lambda_D = 0$ indicates certainty of order. Thus, the wrapping-disorder correlation dictates that a dehydron ($7 < \rho < 19$) occurs with 94% certainty in a region with disorder score $\lambda_D > 0.35$ flanked by well-structured regions ($\lambda_D < 0.35$).[9]

For the 19 tyrosine kinases reported in PDB, the sequence-based dehydron predictions coincide with the structure-based direct identification of the dehydrons. This fact validates our sequence-based packing comparison of human tyrosine kinases, shown in Figure 4. The sequence-based packing comparison between any two kinases is necessarily an overall assessment, not restricted to the ligand binding sites, as such information cannot be reliably obtained unless the kinase−ligand complex is reported in the PDB. Thus, overall packing similarity is *a sufficient but not necessary* condition for cross reactivity (two proteins might have differences in their overall packing, while their ATP pockets are similarly packed).

Table 1. Subfamily and Tyrosine Kinases Numbered According to the Rows and Columns of the Packing Distance Matrix Shown in Figure 4[a]

1	Lmr_LMR1	32	Eph_EphA1 0	63	FGFR_FGF R2*
2	Lmr_LMR2	33	DDR_DDR 1	64	FGFR_FGF R3*
3	Lmr_LMR3	34	DDR_DDR 2	65	FGFR_FGF R1*
4	CCK4_CCK 4	35	Trk_TRKB	66	FGFR_FGF R4
5	Ack_ACK	36	Trk_TRKC	67	Ret_RET
6	Ack_TNK1	37	Trk_TRKA	68	VEGFR_K DR
7	EGFR_EGF R*	38	Musk_MUS K	69	VEGFR_FL T1
8	EGFR_HER 2/ErbB2*	39	Ror_ROR1	70	VEGFR_FL T4
9	EGFR_HER 4/ErbB4	40	Ror_ROR2	71	PDGFR_F MS
10	EGFR_HER 3/ErbB3	41	Abl_ABL*	72	PDGFR_KI T*
11	JakA_JAK1	42	Abl_ARG	73	PDGFR_PD GFRa
12	JakA_TYK2	43	Src_HCK*	74	PDGFR_PD GFRb
13	JakA_JAK2	44	Src_LYN	75	PDGFR_FL T3
14	JakA_JAK3	45	Src_LCK*	76	Tie_TIE2
15	Syk_SYK*	46	Src_BLK	77	Tie_TIE1
16	Syk_ZAP70	47	Src_SRC*	78	Axl_AXL
17	Fak_FAK	48	Src_YES	79	Axl_MER
18	Fak_PYK2	49	Src_FYN*	80	Axl_TYRO 3
19	Eph_EphA3	50	50. Src_FGR	81	Met_MET
20	Eph_EphA5	51	Src_FRK	82	Met_RON
21	Eph_EphA4	52	Src_BRK	83	Ryk_RYK
22	Eph_EphA6	53	Src_SRM	84	Alk_ALK
23	Eph_EphA7	54	Tec_BT K*	85	Alk_LTK
24	Eph_EphB1	55	Tec_BMX	86	Sev_ROS
25	Eph_EphB2	56	Tec_TEC*	87	InsR_INSR*
26	Eph_EphB3	57	Tec_TXK	88	InsR_IGF1 R*
27	Eph_EphB4	58	Tec_ITK	89	InsR_IRR
28	Eph_EphA8*	59	Csk_CSK*	90	JakB_Doma in2_JAK1
29	Eph_EphA2*	60	Csk_CTK	91	JakB_Doma in2_TYK2
30	Eph_EphA1	61	Fer_FER	92	JakB_Doma in2_JAK2
31	Eph_EphB6	62	Fer_FES	93	TK-Unique_ _SuRTK106

[a] The 19 kinases marked with an asterisk are reported in the PDB.

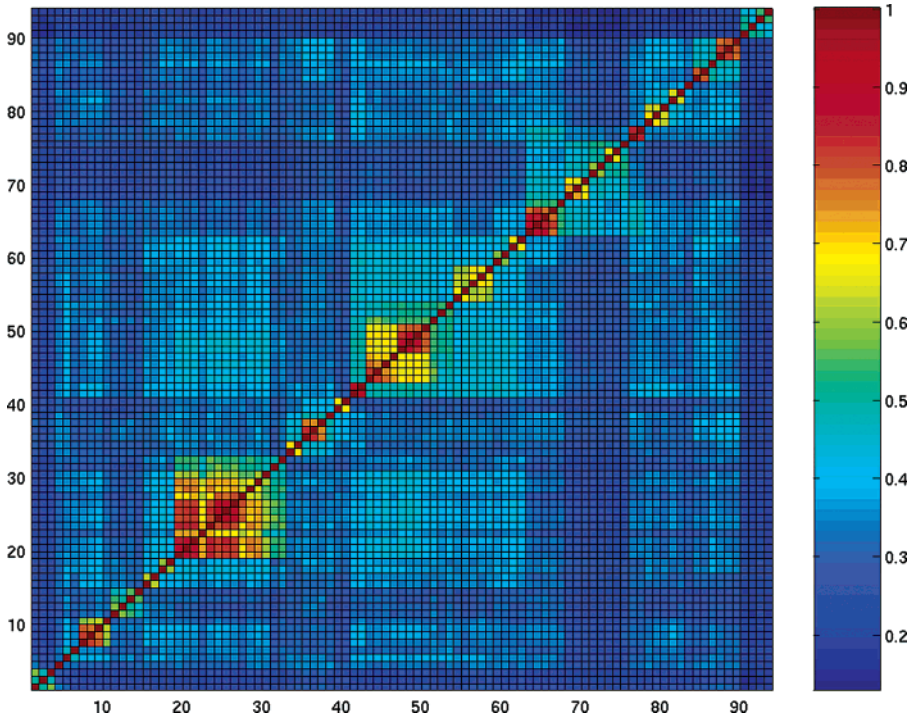

Figure 4. Packing distance matrix over all human tyrosine kinases. The numbering denotes the subfamily and kinase, as indicated in Table 1. In the absence of PDB structure, dehydron patterns were inferred from the disorder−score plot, as indicated in the Methods section.

The predicted correlations emerging from the packing distance matrix (Table 1, Figure 4) call for a pharmacological corroboration. Particularly noteworthy are inferred cross reactivities between the insulin receptor (InsR) and the Abelson (Abl) subfamilies, evocative of the presumed impact of Gleevec on diabetes,[19] and cross reactivities between the following subfamily pairs: Abl-Src (in particular Abl-SRC); Abl-Axl; Abl-Tec; Src_SRC-Src_YES, Src_SRC-Src_FYN, Src_SRC-Src_FGR; FGFR-Tie; VEGFR-PDGFR_FLT3; Alk-InsR; VEGFR-Tie_TIE1.

Proof of Concept: Drug Redesign from Packing-Based Cross-Reactivity Predictions. Test tube evidence pointing to the feasibility of a packing-based cross-reactivity predictor has been presented elsewhere.[20] Thus, the inhibitory impact of the

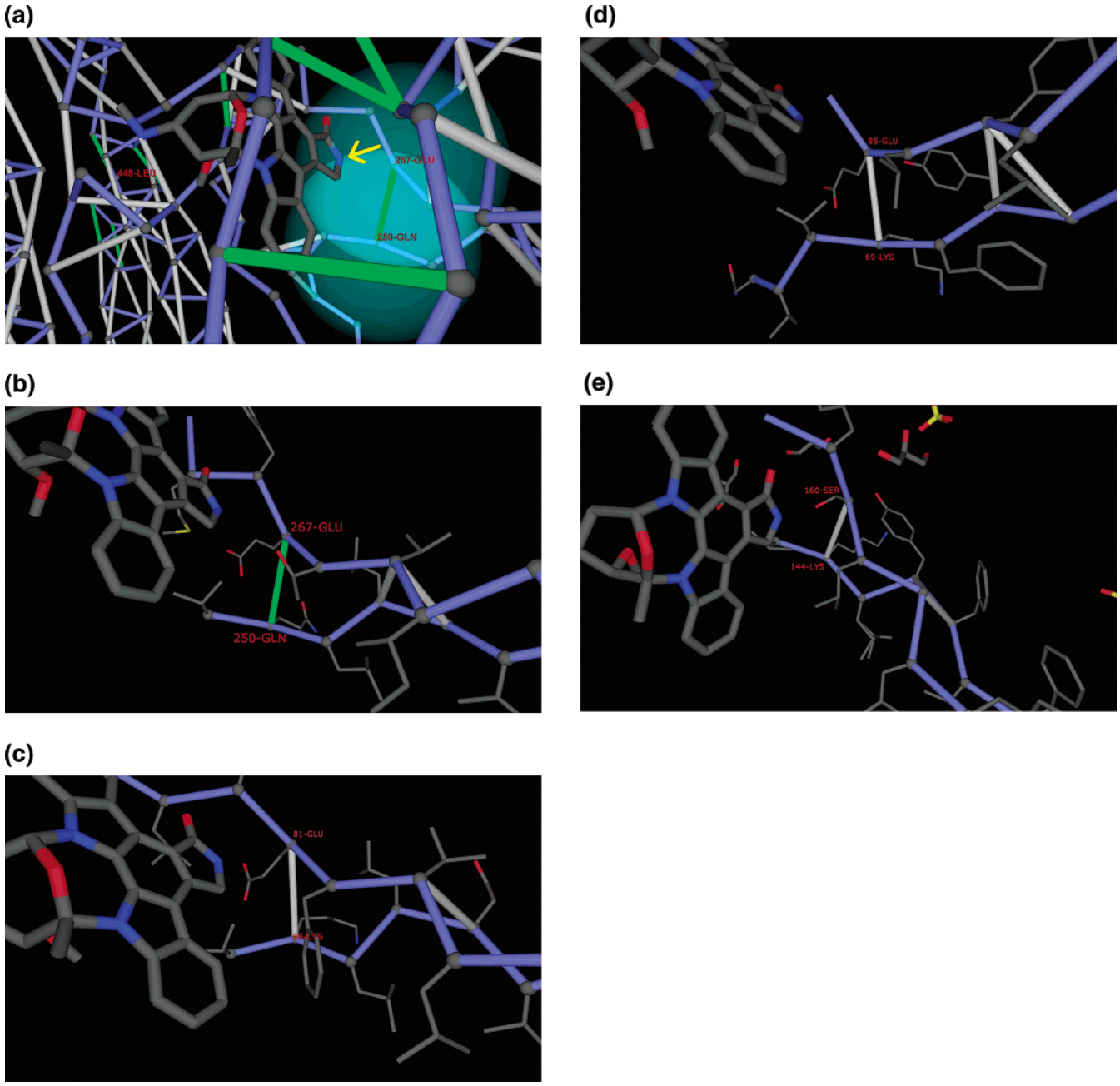

Figure 5. Relative position of kinase packing defects around the ligand indole region in staurosporine−kinase complexes. (a) Microenvironment of dehydron Gln250−Glu267 in Src kinase framed by the desolvation spheres centered at the α-carbons of Gln250 and Glu267. Methylation at the indole N5-position (indicated by the arrow) would turn the ligand into a wrapper of the packing defect in Src kinase. (b) Simplified view of the ligand position with respect to the Gln250−Glu267 dehydron in Src kinase. (c) Wrapping environment of the dehydrated backbone hydrogen bond Lys65−Glu81 in CDK2 which aligns with dehydron Gln250−Glu267 in Src kinase. (d) Idem for dehydrated hydrogen bond Lys69−Glu85 in Chk1. (e) Idem for dehydrated hydrogen bond Lys144−Ser160 in PDK1.

cancer therapeutic drug Gleevec has been sharpened, taking into account packing differences across its targets[20] and modifying the parental compound accordingly. In this way, the differences between packing and pharmacological distances among Gleevec targets may be significantly reduced.

A much more stringent test involves redesigning *staurosporine*, the most promiscuous kinase ligand,[7] in order to elicit a selective inhibitory impact that reflects packing differences and thus distinguishes one target from the others. Thus, four PDB-reported staurosporine-binding kinases with significant pairwise packing distances (>0.4) and extremely low staurosporine-based pharmacological distance (<0.01) may be considered: Src kinase (PDB.1BYG), CDK2 (PDB.1AQ1), Chk1 (PDB.1NVR) and PDK1 (PDB.1OKY). Our wrapping analysis reveals that only the Src kinase possesses a nonconserved dehydron, the backbone hydrogen bond Gln250−Glu267, that may be wrapped exogenously by methylating staurosporine at the imide N6-position of the indole ring (Figure 5a). Upon structural alignment, we can see that the Src dehydron maps into the well-wrapped backbone hydrogen bonds Lys65−Glu81 in CDK2, Lys69−Glu85 in Chk1, and Lys144−Ser160 in PDK1 (Figure 5). Thus, we predict that selectivity for Src kinase may be achieved by redesigning staurosporine to turn it into a wrapper of the Gln250−Glu267 dehydron, a packing defect *not* conserved in alternative targets CDK2, Chk1, and PDK1, of the parental compound.

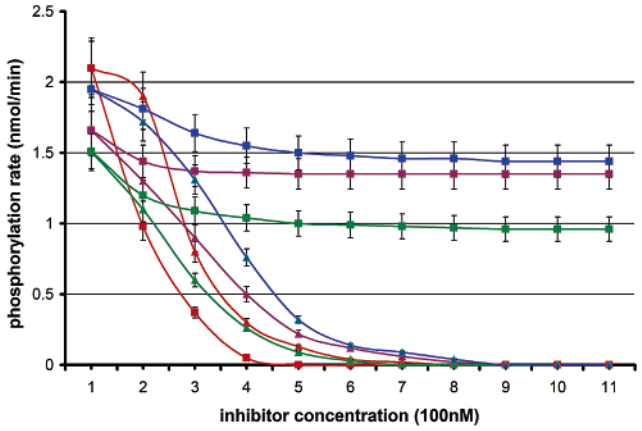

Figure 6. Phosphorylation rates of Src (red), CDK2 (blue), Chk1 (purple), and Pdk1 (green) in the presence of staurosporine (triangles) and in the presence of the staurosporine methylated at the imide N6 of the indole ring (squares). The latter compound was designed to better wrap the nonconserved dehydron Gln250−Glu267 in Src kinase. Error bars represent dispersion over 8 runs of each kinetic assay. Within the means of detection, the kinase phosphorylation rates do not vary appreciably in the range 0−100 nM inhibitor concentration.

The redesign[21,22] of staurosporine entails replacing the imide hydrogen in the indole ring with a methyl group, a substitution known to severely impair the capacity of the ligand to become engaged as donor in an intermolecular hydrogen bond with the ATP pocket (Figure 5b,c,e).[23] Methylation at indole N6 may be achieved by several routes: (a) recapitulating the staurosporine synthesis using methyl substitution on the indole N6 as protective group, and retaining the substitution throughout the synthesis; (b) using staurosporine as the starting point and methylating with NaH/DMF (sodium hydride/dimethyl formamide) with prior protection of alternative N-methylation sites;[23] and (c) following the short pathway based on intramolecular Diels−Alder reaction of pyrano[4,3-*b*]indol-3-one, described in ref 23, page 4399, replacing the first step by treatment of commercial 2-nitrocinnamaldehyde with 1,2-dimethyl hydrazine (for indole N6 methylation) instead of hydrazine. The latter route was chosen for simplicity. The yield of the first synthetic step increases from 58% to 71% as hydrazine is replaced by 1,2-dimethyl hydrazine, in accord with the difference in indole protection.

To test whether the specificity and affinity for Src improved as the staurosporine derivative is compared with the parental compound, we conducted a kinetic spectrophotometric assay.[24] This assay was geared at measuring the phosphorylation rate of peptide substrates[25−28] in the presence of the kinase inhibitor at different concentrations. As indicated in Figure 6, the inhibition of the Src by the drug-wrapper of dehydron Gln250−Glu267 *improved* when compared with the parental staurosporine (Sigma-Aldrich) level. Furthermore, the inhibitory impact of the ligand-wrapper in the form of a methylated staurosporine derivative became *selective* for Src vis-à-vis CDK2, Chk1, and PDK1. Dehydron Gln250−Glu267 is absent in the latter PDB-reported kinases, and consistently, the drug designed to better wrap it has very low inhibitory impact against the other paralog kinases. Thus, we have shown that packing differences across protein paralogs may be used to achieve specificity by suitably modifying even the most promiscuous kinase inhibitor.

Conclusions

As the example of Gleevec attests,[2,13,14] drug selectivity is not invariably necessary for activity. However, the assessment of cross reactivity and the resulting side effects is a critical issue in drug-based inhibition of kinase function. This work introduces a structural marker, the packing defect or dehydron, that enables the a priori inference of cross reactivity. Our inferences are validated by independent high-throughput affinity fingerprinting of kinases. We showed that the a priori inference of drug cross reactivity based on protein packing differences constitutes a design tool to guide the modulation of selectivity as needed for parallel inhibition of multiple targets as well as for sharpening the inhibitory impact of lead compounds.

Other molecular attributes have failed to provide a basis for cross reactivity prediction. For instance, distance in sequence space does not correlate significantly with pharmacological distance,[10] nor do hydrophobicity differences at the ATP site:[20] binding sites tend to have an average hydrophobicity not significantly higher than the rest of the protein surface.

Our structure-based methodology to confine the inhibitory impact and ultimately optimize the therapeutic index can be extended to any universe of purported protein targets, provided some members of the superfamily are reported in the PDB. In the absence of structure it is still possible to infer packing defects through a strong correlation between hydrogen-bond wrapping and disorder score, an accurate sequence-based attribute.[9] The latter parameter indicates the propensity of a peptide-chain window to be conformationally disordered, and the correlation arises because the inability to protect intramolecular hydrogen bonds from water attack is causative of disorder.[9] Furthermore, provided some target structures are available, the spatial location of predicted packing defects in other a priori targets may be obtained from structure threading or homologue modeling.[9] This procedure is facilitated by the fact that paralog structures are considerably aligned. Thus, packing distances, and hence cross reactivities, may be inferred provided a few structures for paralog targets are reported.

Methods

Dehydron Identification. A dehydron is identified by determining the extent of intramolecular desolvation, ρ, of the hydrogen bond, quantified as the number of the side chain carbonaceous nonpolar groups that lie within the desolvation domain the hydrogen bond. The desolvation domain consists of two intersecting balls of radius 6.4 Å centered at the α-carbons of the hydrogen-bond-paired residues. In folds for soluble proteins at least two-thirds of the backbone hydrogen bonds are wrapped on average by $\rho = 26.6 \pm 7.5$ nonpolar groups.[8,9] Dehydrons are then defined as hydrogen bonds whose extent of wrapping lies in the tails of the distribution, i.e., with 19 or fewer nonpolar groups in their desolvation domains, so their ρ-value is below the mean, minus one Gaussian dispersion.

Packing Distance. For a protein chain of length N, a matrix of dehydrons or underwrapped H-bonds D_{ij}, $i, j = 1, 2, ..., N$, is constructed by choosing $D_{ij} = 1$ if residues i and j are paired by a dehydron and $D_{ij} = 0$ otherwise. Then a Hamming distance $M_H(X, Y)$, which serves as an indicator of the packing distance between proteins X and Y, is given by

$$M_H(X, Y) = \sum_{i<j} |\mathbf{D}_{i,j}(X) - \mathbf{D}_{i,j}(Y)|$$

where $\mathbf{D}(X)$ and $\mathbf{D}(Y)$ represent, respectively, the dehydron matrices for proteins X and Y. In comparing kinases for pharmacological purposes, the Hamming distance is restricted to those residues that belong to the hulls, that is, to the residues that frame the microenvironments of the hydrogen bonds within the ATP-binding site.

Pharmacological Matrix. The pharmacological distance between two kinases is defined as the Euclidean distance between the normalized affinity vectors with entries corresponding to the

negative logarithm of the binding constants reported in Fabian et al.[7] The pharmacological matrix (**PM**) is obtained by calculating the pharmacological distances between all the pairs of 32 kinases:

$$\mathbf{PM}_{X,Y} = ||X - Y|| = \sqrt{\sum_{n \in \text{set of inhibitors}} (X_n - Y_n)^2}$$

where X_n and Y_n represent, respectively, the normalized values of the negative logarithm of binding constants for complexation of kinase *X* and kinase *Y* with drug inhibitor *n*.

Structural Alignment. The 3D structural alignment of the kinase complexes with their inhibitors, adopted to determine the inhibitor hull, is performed using the Cn3D program.[29]

Sequence-Based Dehydron Prediction. A relationship has been established[9] between wrapping and a structural parameter that may be reliably predicted from sequence: the propensity for inherent structural disorder in any region of a monomeric fold.[18] This parameter is assessed with high degree of accuracy by the program PONDR, a neural-network predictor of native disorder. Only 0.4% of more than 900 nonhomologous PDB proteins give false positive predictions in regions with 40 or more consecutive sites of predicted disorder. Even this 0.4% of false positives is an overestimation, as many disordered regions in monomeric chains become ordered upon ligand binding or in crystal contacts.[9] The false negatives error rate (~11% for regions of 40 or more consecutive predicted ordered residues) is also compelling in regards to the predictor quality.

The correlation between wrapping and disorder propensity implies that it is possible to predict dehydrons directly from sequence:[9] It suffices to determine the PONDR-generated pattern corresponding to each of the desired features. The correlation implies that the propensity to adopt a natively disordered state becomes pronounced for proteins which, due to a chain composition reflecting high hydrophilicity, cannot fulfill the minimal wrapping requirement for the protection of their backbone hydrogen bonds. This minimal requirement dictates that at least seven nonpolar groups should wrap each backbone hydrogen bond.[9] The correlation between disorder score at a particular residue site and the extent of wrapping of the hydrogen bond engaging that residue is presented in ref 9.

The strong correlation implies that we can infer the existence of dehydron-rich regions from the PONDR score (λ_d) with 92% accuracy in regions with $\lambda_d > 0.35$ provided such regions are flanked by well-wrapped regions ($\lambda_d < 0.35$), to ensure the actual existence of structure. The accuracy of the sequence-based dehydron predictor[9] was established by inferring the location of dehydrons in proteins with reported structure, for which the wrapping of each hydrogen bond can be calculated directly. The false negatives constitute 368 of the 8215 dehydrons in a PDB database of 1466 proteins free from structural redundancy and less than 25% sequence identity in pairwise alignment. The false positives correspond to 2721 of the 133 623 backbone hydrogen bonds examined.

Spectrophotometric Kinetic Assay. To determine the level of selectivity of drug inhibitors designed by adopting the wrapping technology, kinetic assays of the inhibition of multiple kinases have been conducted. To measure the rate of phosphorylation due to kinase activity in the presence of inhibitors, a standard spectrophotometric assay has been adopted[24] in which the adenosine diphosphate production is coupled to the NADH oxidation and determined by absorbance reduction at 340 nm. Reactions were carried out at 35 °C in 500 μL of buffer (100 mM Tris-HCl, 10 mM $MgCl_2$, 0.75 mM ATP, 1 mM phosphoenol pyruvate, 0.33 mM NADH, 95 units/mL pyruvate kinase, pH 7.5). The following peptide substrates (Invitrogen/Biaffin) for kinase phosphorylation were chosen for their high specificity: KVEKIGEGTYGVVYK for Src,[25] HHASPRK for CDK2,[26] GCSPALKRSHSDSLDHDIFQL for Chk1,[27] and EGLGPGDTTSTFCGTPNYIAP for Pdk1.[28]

Acknowledgment. The research of A.F. is supported by NIH Grant 1R01 GM072614-01A1 from the National Institute of General Medical Sciences. Early stages of the work were supported by an unrestricted grant from Eli Lilly and Company awarded to A.F. We emphatically thank Dr. Kristina Rogale for help with the automated computation of packing distances, Prof. William Bornmann for his advice on organic synthesis of staurosporine derivatives, and Prof. Axel Blau for his help with the kinetic assays. We thank Drs. Chen Su and Harry Harlow (Lilly) for their valuable input to this research.

References

(1) Taylor, S. S.; Radzio-Andzelm, E. Protein kinase inhibition: natural and synthetic variations on a theme. *Curr. Opin. Chem. Biol*. **1997**, *1*, 219−226.
(2) Donato, N. J.; Talpaz, M. Clinical use of tyrosine kinase inhibitors: Therapy for chronic myelogenous leukemia and other cancers. *Clin. Cancer Res.* **2000**, *6*, 2965−66.
(3) Dancey, J.; Sausville, E. A. Issues and progress with protein kinase inhibitors for cancer treatment. *Nat. Rev. Drug Discovery* **2003**, *2*, 296−313.
(4) Fabbro, D.; Garcia-Echeverria C. G. Targeting protein kinases in cancer therapy. *Curr. Opin. Drug Discovery Dev.* **2002**, *5*, 701−712.
(5) Gabriele, A.; King, G. L. Protein kinase C inhibitors in the treatment and prevention of diabetic complications. *Curr. Opin. Endocrinol. Diabetes* **2001**, *8*, 197−204.
(6) Myers, M. R.; He, W.; Hulme, C. Inhibitors of tyrosine kinases involved in inflammation and autoimmune disease. *Curr. Pharm. Des.* **1997**, *3*, 473−502.
(7) Fabian, M. A. et al. A small molecule kinase interaction map for clinical kinase inhibitors. *Nat. Biotechnol.* **2005**, *23*, 329−336.
(8) Fernández, A.; Rogale, K.; Scott, R. L.; Scheraga, H. A. Inhibitor design by wrapping packing defects in HIV-1 proteins. *Proc. Natl. Acad. Sci. U.S.A.* **2004**, *101*, 11640−11645.
(9) Fernández, A.; Berry R. S. Molecular dimension explored in evolution to promote proteomic complexity. *Proc. Natl. Acad. Sci. U.S.A.* **2004**, *101*, 13460−13465.
(10) Vieth, M.; Higgs, R. E.; Robertson, D. H.; Shapiro, M.; Gragg, E. A.; Hemmerle, H. Kinomics-structural biology and chemogenomics of kinase inhibitors and targets. *Biochim. Biophys. Acta* **2004**, *1697*, 243−257.
(11) Fernández, A. Keeping dry and crossing membranes. *Nat. Biotechnol.* **2004**, *22*, 1081−1085.
(12) Attoub, S.; Rivat, C.; Rodrigues, S.; Van Borexlaer, S.; Bedin, M.; Buyneel, E.; Louvet, C., et al. The c-kit tyrosine kinase inhibitor STI-571 for colorectal cancer therapy. *Cancer Res.* **2002**, *62*, 4879−4883.
(13) Skene, R. J.; Kraus, M. L.; Scheibe, D. N.; Snell, G. P.; Zou, H.; Sang, B. C.; Wilson, K. P. Structural basis for autoinhibition and STI-571 inhibition of C-kit Tyrosine kinase. *J. Biol. Chem.* **2004**, *279*, 31655−31663.
(14) Cohen, P. Protein kinases − the major drug targets of the twenty-first century? *Nat. Rev. Drug Discovery* **2002**, *1*, 309−315.
(15) Morin, M. From oncogene to drug: development of small molecule tyrosine kinase inhibitors as anti-tumor and anti-angiogenic agents. *Oncogene* **2000**, *19*, 6574−6583.
(16) Mendel, D. B.; Laird, A. D.; Xin, X.; Louie, S. G.; Christensen, J. G.; Li, G.; Schreck, R. E.; Abrams, T. J.; Ngai, T. J.; Lee, L. B.; Murray, L. J.; Carver, J.; Chan, E.; Moss, K. G.; Haznedar, J. O.; Sukbuntherng, J.; Blake, R. A.; Sun, L.; Tang, C.; Miller, T.; Shirazian, S.; McMahon, G.; Cherrington, J. M. In vivo antitumor activity of SU11248, a novel tyrosine kinase inhibitor targeting vascular endothelial growth factor and platelet-derived growth factor receptors: determination of a pharmacokinetic/pharmacodynamic relationship. *Clin. Cancer Res*. **2003**, *9*, 327−337.
(17) Torrance, C. J.; Jackson, P. E.; Montgomery, E.; Kinzler, K. W.; Vogelstein, B.; Wissner, A.; Nunes, M.; Frost, P.; Discafani, C. M. Combinatorial chemoprevention of intestinal neoplasia. *Nat. Med.* **2000**, *6*, 1024.
(18) Braken, C.; Iakoucheva, L. M.; Romero, P. R.; Dunker, A. K. Combining prediction, computation and experiment for the characterization of protein disorder. *Curr. Opin. Struct. Biol.* **2004**, *14*, 570−576.
(19) Couzin, J. Researchers puzzle over possible effect of Gleevec. *Science* **2005**, *307*, 1711
(20) Fernández, A. Incomplete protein packing as a selectivity filter in drug design. *Structure* **2005**, *13*, 1829−1836
(21) Link, J. T.; Raghavan, S.; Danishefsky, S. J. First total synthesis of staurosporine and *ent*-staurosporine. *J. Am. Chem. Soc*. **1995**, *117*, 552−553.
(22) Bregman, H.; Williams, D. S.; Atilla, G. E.; Carroll, P. J.; Meggers, E. An organometallic inhibitor for glycogen synthase kinase 3. *J. Am. Chem. Soc.* **2004**, *126*, 13594−13595.

(23) Knölker, H. J.; Reddy, K. R. Isolation and synthesis of biologically active carbazole alkaloids. *Chem. Rev.* **2002**, *102*, 4303−4427.
(24) Schindler, T.; Bornmann, W.; Pellicena, P.; Miller, W. T.; Clarkson, B.; Kuriyan, J. Structural mechanism for STI-571 inhibition of abelson tyrosine kinase. *Science* **2000**, *289*, 1938−1942.
(25) Cheng H. C.; Nishio H.; Hatase O.; Ralph S.; Wang J. H. A synthetic peptide derived from p34cdc2 is a specific and efficient substrate of src-family tyrosine kinases. *J. Biol. Chem.* **1992**, *267*, 9248−56.
(26) Brown N. R.; Noble M. E.; Endicott J. A.; Johnson L. N. The structural basis for specificity of substrate and recruitment peptides for cyclin-dependent kinases. *Nat. Cell. Biol.* **1999**, *7*, 438−43.
(27) O'Neill T.; Giarratani L. et al. Determination of substrate motifs for human Chk1 and hCds1/Chk2 by the oriented peptide library approach. *J. Biol. Chem.* **2002**, *277*, 16102−15.
(28) Le Good, J. A.; Ziegler, W. H.; Parekh, D. B.; Alessi, D. R.; Cohen, P.; Parker, P. J. Protein kinase C isotypes controlled by phosphoinositide 3-kinase through the protein kinase PDK1. *Science* **1998**, *281*, 2042−2045.
(29) Hogue, C. W. V. Cn3D: a new generation of three-dimensional molecular structure viewer. *Trends Biochem. Sci.* **1997**, *22*, 314−316.

JM060163J